EUROPHYSICS LETTERS 1 September 2001

Europhys. Lett., **55** (5), pp. 719–725 (2001)

Disorder-induced roughening transition of many elastic lines in a periodic potential

T. KNETTER[1,2], G. SCHRÖDER[1,2], M. J. ALAVA[3] and H. RIEGER[4]

[1] *Institut für Theoretische Physik, Universität zu Köln - 50926 Köln, Germany*
[2] *NIC c/o Forschungszentrum Jülich - 52425 Jülich, Germany*
[3] *Helsinki University of Technology, Laboratory of Physics*
P.O. Box 1100, 02015 HUT, Finland
[4] *Theoretische Physik, Universität des Saarlandes - 66041 Saarbrücken, Germany*

(received 4 January 2001; accepted in final form 14 June 2001)

PACS. 74.60.Ge – Flux pinning, flux creep, and flux-line lattice dynamics.
PACS. 68.35.Ct – Interface structure and roughness.
PACS. 68.35.Rh – Phase transitions and critical phenomena.

Abstract. – The competing effect of a periodic pinning potential and random point disorder is studied for ensembles of elastic lines or directed polymers. The ground states are investigated by exact combinatorial optimization. In both two and three dimensions a phase diagram is found with two or three distinct phases: a strictly flat phase if the disorder is bounded and weak, a weakly fluctuating phase for intermediate valley depths, where the lines roughen individually on a scale smaller than the line-line distance, and a rough phase for strong disorder, where the roughness follows the scaling with pure point disorder. In the three-dimensional, rough phase the line wandering in the transverse direction leads to an entangled state with a complicated topology.

Ensembles of elastic lines form one of the most interesting examples of the interplay of disorder and an ordering tendency. Much of the attention is motivated by the experimental connections to dirty type-II superconductors, in which flux lines (FL) interact with point or columnar defects [1–3]. This interaction often gives rise to beneficial, technologically important effects since the impurities pin lines, individually or collectively, and creating them in a controlled fashion has been demonstrated by various techniques. The theory of FL arrays with a wide variety of possible disorder backgrounds has received great interest [4]. It is worth noting that the physics of a single FL has connections to paradigmatic questions in non-equilibrium statistical mechanics [5,6] through mappings to the Kardar-Parisi-Zhang equation of kinetic roughening in surfaces, and to Burgers' equation of vortex-free turbulence [7].

Here we analyze with exact numerical tools the roughening or disordering of an ensemble of elastic lines at zero temperature when point disorder competes with a periodic potential that tries to order the ensemble into a regular structure. The FL analogue is the Abrikosov lattice in the presence of point disorder. For both the two- and the three-dimensional case ($2d$ and $3d$) we find a transitions in terms of the ratio $q = [\epsilon]_{\rm av}/\Delta$, where Δ measures the depth of the potential valleys, and $[\epsilon]_{\rm av}$ is the average strength of the point disorder.

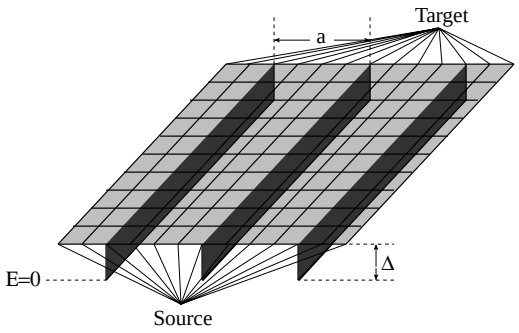

Fig. 1 – Periodic potential in $2d$. The depth of the valleys is denoted by Δ and the nearest-neighbour distance by a. In the model there is additional point disorder ϵ, which is not shown. The FL can only enter and leave the system via the energetically neutral arcs connecting the source and the sink, respectively, with the potential valleys.

Below a *roughening transition* threshold q_{c_2} the lines behave like individual lines in the presence of columnar defects, and bulk disorder [8]. The fluctuations are restricted in the transverse direction, thus making the line-to-line interaction negligble. For unbounded disorder, this phase extends down to zero disorder strength, whereas for bounded disorder we have an intermediate flat region ($q < q_{c_1}$) in which the lines are strictly confined to the potential valleys. Above the roughening transition ($q \geq q_{c_2}$) there is a crossover to the asymptotic roughness of multiline systems, which is expected in systems without the periodic potential [9]. This is accompanied by an *entangled state* in three dimensions since in the asymptotic, large system size limit the lines have freedom to move in the transverse direction.

We are interested in an assembly of N elastic lines described by the Hamiltonian

$$\mathcal{H} = \sum_{i=1}^{N} \int_0^H \mathrm{d}z \left\{ \frac{\gamma}{2} \left[\frac{\mathrm{d}\boldsymbol{r}_i}{\mathrm{d}z} \right]^2 + \sum_{j(\neq i)} V_{\mathrm{int}}[\boldsymbol{r}_i(z) - \boldsymbol{r}_j(z)] + V_r[\boldsymbol{r}_i(z), z] + V_{\mathrm{p}}[\boldsymbol{r}_i(z)] \right\} , \quad (1)$$

where the vectors $\boldsymbol{r}_i(z) \in \mathcal{R}^{d-1}$ (with $d = 2$ and $d = 3$ studied here) denote the transverse displacement of the i-th line at longitudinal coordinate z; H is the system height; $V_r[\boldsymbol{r}, z]$ describes the point disorder, which is taken to be delta-correlated with variance ϵ; $V_{\mathrm{int}}[\boldsymbol{r} - \boldsymbol{r}']$ is a short-range repulsive interaction between the lines (*e.g.* hard-core) and $V_{\mathrm{p}}[\boldsymbol{r}]$ a periodic potential with period a in all transverse space directions. We assume its minima to be well localized, *i.e.* they have a width that is small compared to the interaction range of the lines. This allows only single occupancy of the potential valleys and we concentrate on the case in which the line density ($\rho = L^{d-1}/N$) is such that each potential valley is occupied by exactly one elastic line, *i.e.* $\rho = 1/a^{d-1}$. A similar model has been studied in $d = 1 + 1$ in [10] for the competition between point disorder and random columnar defects, *i.e.* a potential V_{p} that is not periodic but random.

We study a lattice version of the continuum model equation (1) which is defined [11] on a square lattice of size $L^{d-1} \times H$. To each bond (ij) of the lattice an energy $e_{ij} = \epsilon_{ij} + \Delta_{ij}$ is assigned. Along longitudinal, periodically arranged lines of the lattice Δ_{ij} is set to zero, whereas it equals a positive value Δ for all other bonds of the lattice. These lines form the potential valleys of effective depths $-\Delta$, cf. fig. 1. Additionally, point disorder is introduced to the model by adding a random number ϵ_{ij} to each lattice bond. The investigated distribution of ϵ_{ij} are i) the uniform distribution (bounded disorder) $P(\epsilon) = 1$ for $0 \leq \epsilon \leq \epsilon_{\max}$ and

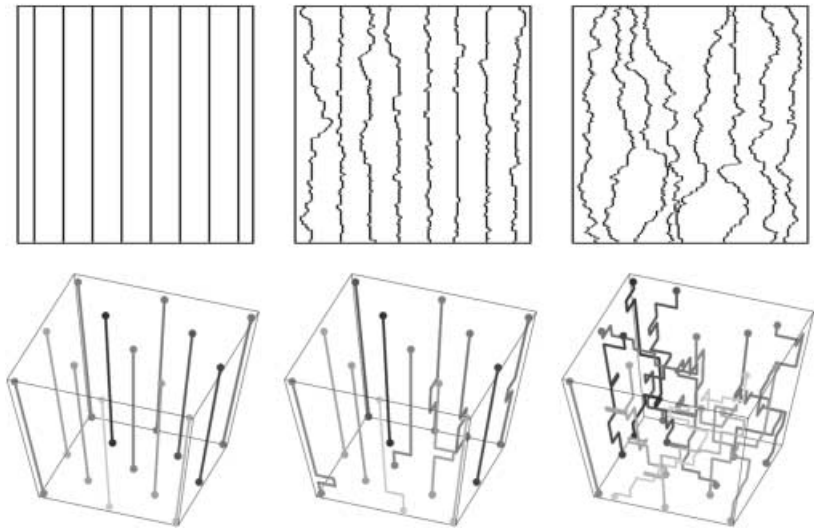

Fig. 2 – Optimal ground-state configurations in $2d$ (top) and $3d$ (bottom) for different point disorder strengths, q, increasing from left to right. In the flat phase (left) the FLs are trapped completely inside the potential valleys.

$P(\epsilon) = 0$ otherwise, and ii) the exponential distribution (unbounded disorder) $P(\epsilon) = \exp[-\epsilon]$ for $\epsilon \geq 0$ and $P(\epsilon) = 0$ otherwise. The ratio $q = \langle \epsilon_{ij} \rangle / \Delta$ is a measure for the strength of point disorder. The energy e_{ij} is the cost of occupying the lattice bond (ij) by a segment of a FL. The hard-core interaction between FLs is implicitly incorporated by requiring that each bond cannot be occupied by more than one FL. Since all bond energies e_{ij} are positive, short line lengths are more favourable than longer ones which reproduces the elastic energy of the continuum Hamiltonian. The lattice Hamiltonian then reads

$$H(\boldsymbol{x}) = \sum_{(ij)} e_{ij} \cdot x_{ij} \ , \tag{2}$$

where $\sum_{(ij)}$ is a sum over all *arcs* (ij) joining site i and j of a d-dimensional, *e.g.* rectangular $(L^{d-1} \times H)$ lattice, with open boundary conditions (b.c.) in all space directions. For convenience we consider forward and backward arcs such that for each pair of sites i, j there is a bond (ij) *and* a bond (ji). The FLs enter the system via the plane $z = 0$ and leave it via the plane $z = H$, see fig. 1. The FL configuration is defined by the set of variables x_{ij} that are either 0 or 1: $x_{ij} = 1$ if a FL runs from site i to j, $x_{ij} = 0$ otherwise. For the configuration to form *lines* on each site of the lattice, the configuration $\boldsymbol{x}$ has to be divergence free, *i.e.* $\forall i : \nabla_i \boldsymbol{x} \equiv \sum_{j \text{ n.n. of } i} x_{ji} - \sum_{j \text{ n.n. of } i} x_{ij} = 0$. All sites of the top (bottom) lattice plane are attached to an additional ghost site s (t) via energetically neutral arcs. The lattice divergence of these two sites is required to be $\nabla_s x = 0$ and $\nabla_t x = 0$, respectively, where N is the number of FLs. Finding the minimum energy configuration of N lines now becomes equivalent to a *minimum cost flow problem* with energy function (2) and the mass balance constraints expressed in the site divergences. This task can be solved exactly in polynomial time (with complexity $\mathcal{O}(N \cdot L^{d-1} H)$ by applying the successive-shortest-path algorithm which is described in detail in [11–13]).

Figure 2 demonstrates with a series of snapshots the geometry involved in the calculations,

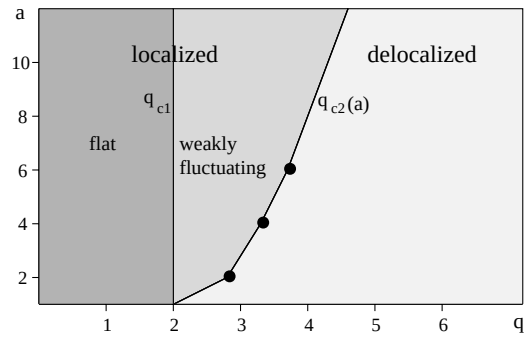

Fig. 3 – Schematic phase diagram in $2d$ for bounded disorder. The full circles correspond to the numerical estimates of the critical disorder strength q_{c_2}, where the roughening transition occurs, for a given period of the peridiodic potential. Below $q = q_{c_1} \approx 2$ all lines are strictly localized to the potential valleys of the periodic potential, independent of *a and* independent of the dimension d.

and the typical behavior with increasing q in $2d$ and $3d$. In both cases the lines are pinned to the energetically favorable valleys for small q, and finally for large q a crossover to a rough state takes place. In $3d$ one can observe that the lines wander almost freely in such conditions. The examples of fig. 2 represent different regions in the a-q phase diagram, which is depicted for $2d$ in fig. 3.

We discriminate between the different regions in the phase diagram by looking at the behavior of the average transverse fluctuation or *roughness* w of the lines [14]:

$$w^2(L,H) = \left[\frac{1}{N} \sum_{i=1}^{N} \frac{1}{H} \int_0^H \mathrm{d}z \left(\boldsymbol{r}_i(z) - \overline{\boldsymbol{r}}_i \right)^2 \right]_{\mathrm{av}} , \tag{3}$$

where $\overline{\boldsymbol{r}}_i = H^{-1} \int_0^H \mathrm{d}z\, \boldsymbol{r}_i(z)$ and $[\ldots]_{\mathrm{av}}$ denotes the disorder average. By studying very large longitudinal system sizes $H \geq 10^4$ we are able to extract the saturation roughness $w(L) = \lim_{H\to\infty} w(L,H)$ for a finite system of transverse size L. Note that we have chosen open b.c.: the transverse fluctuations cannot get larger than the system size. Other quantities of interest are the size $l_\parallel$ of the longitudinal excursions (the average distance between the locations at which a line leaves a valley and returns to it); and the total number of potential valleys PV that a line visits between its entry and terminal point in the limit $H \to \infty$.

Figure 4 displays our data for the roughness w and $l_\parallel$ as a function of $1/q$ in $2d$, fig. 5 displays w and PV in $3d$; both for bounded disorder. In fig. 6 we show our data for w for unbounded disorder. The physical picture that emerges is the following. In the *flat region* we observe $w(L) = 0$, $l_\parallel = 0$ and $PV = 1$, *i.e.* the lines lie completely in the potential valleys. This region ($q < q_{c_1}$) exists only for *bounded* disorder. For the uniform distribution no energetically favourable transverse fluctuation can exist as long as $q < \Delta$. That $q_{c_1} > 1$ follows from the fact that the system is at full occupancy, $N = N_{\mathrm{V}}$, where N_{V} is the number of valleys. For $q \leq q_{c_1}$ the ground state always consists of N straight lines regardless of dimension. The value of q_{c_1} depends on the distance between the valleys and on the disorder distribution (for a flat distribution $q_{c_1} \approx 2$) and is independent of dimension. For *unbounded* disorder this flat region does not exist, since the probability for a repulsive sequence of high-energy bonds in the valleys is always positive. In the *weakly fluctuating region* for $q_{c_1} \leq q \leq q_{c_2}$ the lines roughen locally. Here one finds $w > 0$, $l_\parallel > 0$ and $PV = 1$ and that none of these quantities depends

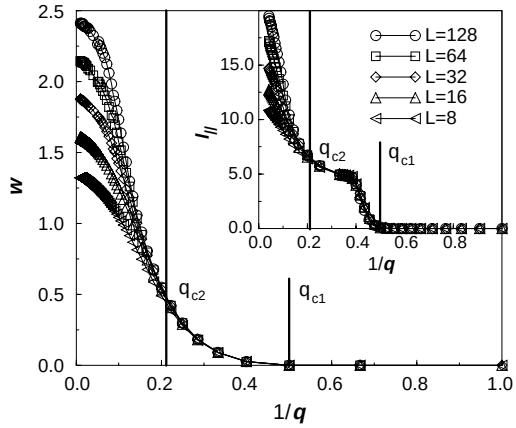

Fig. 4

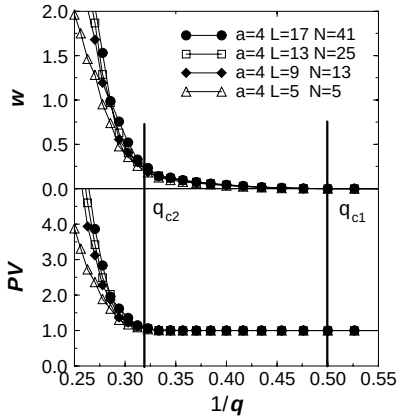

Fig. 5

Fig. 4 – Roughness w in $2d$ as a function of disorder strength q for bounded disorder. q_{c_1} and q_{c_2} are shown. In the flat phase $w = 0$, whereas $w > 0$ for $q > q_{c_1}$. No transversal system size dependence is observered in the weakly fluctuating phase. The inset shows $l_{\|}$. Each data point is averaged over $n = 20$ ($L = 128$) up to $n = 600$ ($L = 8$) disorder configurations, $a = 4$.

Fig. 5 – Top: the same as in fig. 4, now in $3d$. Bottom: the FL start to *jump* from one potential valley to the next at q_{c_2} so that the number of potential valleys each line visits changes from $PV = 1$ to $PV > 1$ at this threshold (bottom). $n = 6$ ($L = 128$) up to $n = 100$ ($L = 5$), $a = 4$.

on the lateral system width. The transverse fluctuations of FLs are bounded by the average line distance or valley separation a. The central feature is that lines fluctuate individually, so that a columnar defect competes with point disorder. Both in $2d$ and in $3d$ a strong columnar pin strictly localizes the line [8] reducing the line-to-line interaction to zero.

With increasing q the transverse fluctuations increase, and when their lengthscale $l_\perp$ becomes comparable to the inter-line distance a the physical properties change. When individual lines can move from one valley to a neighboring valley —*i.e.* exactly when PV becomes larger than unity – the line assembly is collectively rearranged manifesting itself in a system size dependence of the saturation roughness (see fig. 4 for $2d$ and fig. 5 for $3d$). Thus the *rough phase* is characterized by a dependence of w and $l_{\|}$ on the transverse system size and by $PV > 1$. In particular the latter criterion facilitates the numerical determination of the location of the roughness transition at q_{c_2}, which we find to increase monotonically with a.

In the limit $q \to \infty$ the collective behavior of the transverse fluctuations of the lines crosses over to that of a line array in the absence of the periodic potential. The scaling of displacement correlations and the system roughness are slightly decreased compared to the case without the potential because of the lengthscale of the pinned parts of the lines (the remaining tendency to localize in the valleys). For an elastic medium model this would imply that the correlations should depend logarithmically on the distance. In $2d$, in particular, it should be $w \sim \ln L$ and our data indicates indeed (cf. the equidistant data on the y-axis of fig. 4) that the pure disorder scaling is obtained above q_{c_2}.

A fundamental difference exists between the real-space geometry of two-dimensional and three-dimensional systems. In $3d$ and for small line densities, the lines can wander freely since there they can wrap around each other, in contrast to $2d$. This implies that in the thermodynamic limit, the line ensemble becomes *entangled*. We characterize this by computing

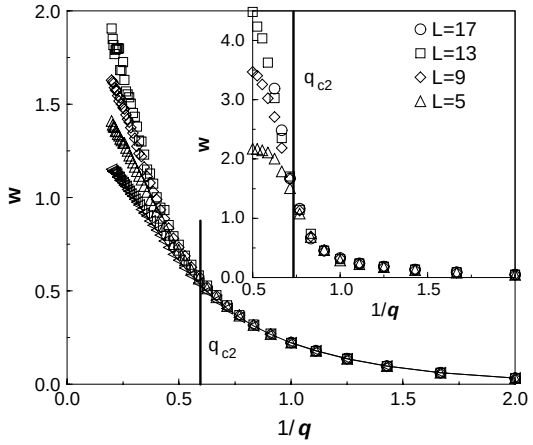

Fig. 6

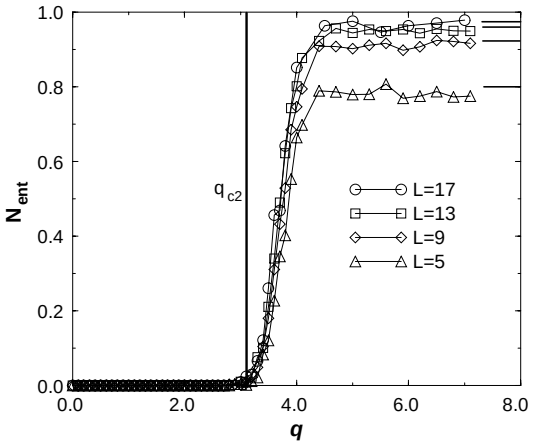

Fig. 7

Fig. 6 – Same as fig. 5 for unbounded disorder. The inset shows $3d$. Though hardly visible from this data, q_{c_1} vanishes. But we still find a finite value of q_{c_2}, below which the roughness shows no L-dependence both in $2d$ and $3d$. $n = 10$ up to $n = 200$, both in $2d$ and $3d$.

Fig. 7 – Number of entangled lines $N_{\rm ent}$ in $3d$ with $a = 4$ normalized by the total number of lines. The horizontal lines indicate the values for completely random permutations of N lines.

the fraction of lines $N_{\rm ent}/N$ that, when forced to start and end in an arbitrary one of all the potential minima, enter and exit in different valleys. In the limits $H \to \infty$, $L \to \infty$ the fraction $N_{\rm ent}(q)/N$ of entangled lines develops a first-order jump at the roughening transition from zero to unity. $N_{\rm ent} = N$ implies that all the lines are entangled, though in a finite system the saturation value of $N_{\rm ent}/N$ is limited by the finite probability that at least one out of N integers ends up at exactly at the same position in a random permutation. This finite-size feature can be seen in the data presented in fig. 7.

When we venture away from the fully occupied case that we have considered here, we expect the roughening transition reported here to vanish. At full occupancy ($\rho = 1$) the fundamental excitations (*e.g.*, jumps of individual lines from one potential valley to the next) have a bulk contribution, due to the full occupancy of the narrow potential valleys. Therefore jumps between valley can occur only if the disorder is strong enough. On the other hand, for $\rho < 1$ empty segments of the potential valleys will allow FLs to jump between them, so that beyond a particular length scale (given by the line density, disorder strength and distance beween the valleys) the FL system is rough. For $\rho > 1$ (*i.e.* all potential valleys are occupied *and* a number of lines are present between the valleys) the system will also be rough, since the lines between the valleys can exchange places without energy loss [9].

To conclude, we have analyzed (with the aid of exact combinatorial optimization methods) ensembles of elastic lines (or directed polymers or FLs) in the presence of a confining periodic potential and competing random point disorder. The main finding is a transition between "rough" and "flat" regimes, in both $2d$ and $3d$, at a finite potential strength. It arises since rare fluctuations are not able to induce line-line interactions when the filling factor of the system is at one. In the rough phase the physics is characterized by correlations that increase with system size. In $3d$ we find an entangled phase, in which the lines form a topologically complicated geometric configuration which will be studied in more detail.

* * *

This work has been supported by the Academy of Finland and the German Academic Exchange Service (DAAD) within a common exchange project, and separately, by the Academy of Finland's Centre of Excellence Programme.

REFERENCES

[1] BLATTER G. *et al.*, *Rev. Mod. Phys.*, **66** (1994) 1125.
[2] NATTERMANN T. and SCHEIDL S., *Adv. Phys.*, **49** (2000) 607.
[3] YOUNG A. P. (Editor), *Spin Glasses and Random Fields* (World Scientific, Singapore) 1997.
[4] FISHER D. S., FISHER M. P. A. and HUSE D. A., *Phys. Rev. B*, **43** (1991) 130; GIAMARCHI T. and LE DOUSSAL P., *Phys. Rev. B*, **52** (1995) 1242.
[5] HALPIN-HEALY T. and ZHANG Y.-C., *Phys. Rep.*, **254** (1995) 215.
[6] LÄSSIG M., *J. Phys. C*, **10** 9905 (1998).
[7] KARDAR M., PARISI G. and ZHANG Y.-C., *Phys. Rev. Lett.*, **56** (1986) 889.
[8] BALENTS L. and KARDAR M. *Phys. Rev. B*, **49** (1994) 13030; HWA T. and NATTERMANN T., *Phys. Rev. B*, **51** (1995) 455.
[9] SCHRÖDER G., KNETTER T., ALAVA M. and RIEGER H., to be published.
[10] HWA T., NELSON D. R. and VINOKUR V. M., *Phys. Rev. B*, **48** (1993) 1167.
[11] RIEGER H., *Phys. Rev. Lett.*, **81** (1998) 4488.
[12] RIEGER H., *Frustrated Systems: Ground State Properties via Combinatorial Optimization, Lect. Notes Phys.*, Vol. **501** (Springer Verlag, Heidelberg) 1998; AHUJA R., MAGNANTI T. and ORLIN J., *Network Flows* (Prentice Hall, New Jersey) 1993.
[13] ALAVA M., DUXBURY P., MOUKARZEL C. and RIEGER H., in *Phase Transitions and Critical Phenomena*, edited by DOMB C. and LEBOWITZ J. L., Vol. **18** (Academic Press, London) 2000, pp. 143-320.
[14] In our model (2) the lines can touch in isolated lattice points; since the hard-core repulsion is only restricted to the lattice bonds, one has to identify the coordinates $\boldsymbol{r}_i(z)$ of the individual lines before calculating the roughness. In $2d$ this is straighforward by ordering them from left to right, in $3d$ we choose the coordinates such that the distance to the lines entry point is minimized. A detailed discussion of the various ways in which lines can be identified in $3d$ including their effect on the values of the average roughness will be presented in [9].